Int. J. Solids Structures Vol. 14, pp. 409–430

0020-7683/78/0601-0409/$02.00/0

UNSTABLE GROWTH OF THERMALLY INDUCED INTERACTING CRACKS IN BRITTLE SOLIDS

S. NEMAT-NASSER, L. M. KEER and K. S. PARIHAR†
The Technological Institute, Northwestern University, Evanston, IL 60201, U.S.A.

(*Received* 26 *September* 1977; *received for publication* 7 *November* 1977)

Abstract—The growth and stability of thermally induced equally spaced parallel cracks in a half-plane consisting of a homogeneous isotropic linearly elastic brittle material are studied. At the initial time, the uniform temperature of the half-plane is reduced at its surface by a large increment, T_0, and then kept constant (at the surface). Because of heat conduction and possible heat convection due to fluid flow, a temperature gradient forms close to the surface and penetrates into the half-plane. Thermal contraction results in the formation of cracks perpendicular to the free surface. It is shown that if the cracks are initially parallel and equally spaced, and if the possibility of branching is excluded, then they grow in time until a critical state is reached. At this state alternate cracks stop growing, while the others begin to grow at a much faster rate. This process continues until another critical state is attained, where the cracks which had stopped growing (together with some other cracks, depending on the temperature profile), suddenly close, while the cracks which have continued growing, suddenly "snap" into a finitely longer length. At this state the crack spacing is doubled (or quadrupled, depending on the temperature profile). The whole process then repeats itself. Applications to geothermal energy extraction from hot dry rock masses is mentioned.

1. INTRODUCTION

In recent years there has been a fair amount of activity in the United States to extract heat energy from hot, dry, impermeable rock masses that exist at relatively shallow depths in mountains in New Mexico; see Smith *et al.*[1]. The basic idea is to induce by hydraulic fracturing a large vertical crack (about, say, a kilometer in diameter) several kilometers below ground surface, and to circulate water down and through the fracture zone and back up to ground surface. In an ideal situation the fracture occurs perpendicular to the smallest principal stress. At the depths and for the location mentioned above, the overburden pressure is considerably larger than the two principal horizontal tectonic stresses, resulting in the formation of a fracture perpendicular to the smallest horizontal principal stress. The local anisotropy and inhomogeneity can considerably influence the final crack orientation. As the rock is cooled by the circulating water, thermally induced secondary cracks may form perpendicular to the face of the primary crack. Since the horizontal principal stress is considerably smaller than the overburden stress, the secondary cracks will probably assume vertically elongated hexagonal shapes. In the limiting case, when the overburden pressure is suitably large, the secondary cracks may constitute a system of vertical parallel cracks. Since the elastic energy stored in the rock by thermal contraction is finite, there will be a finite number of cracks per unit length in the x-direction (see Fig. 1c) with a calculable minimum average crack spacing at the initial stage. As the rock is further cooled, the secondary cracks will penetrate deeper into the rock.

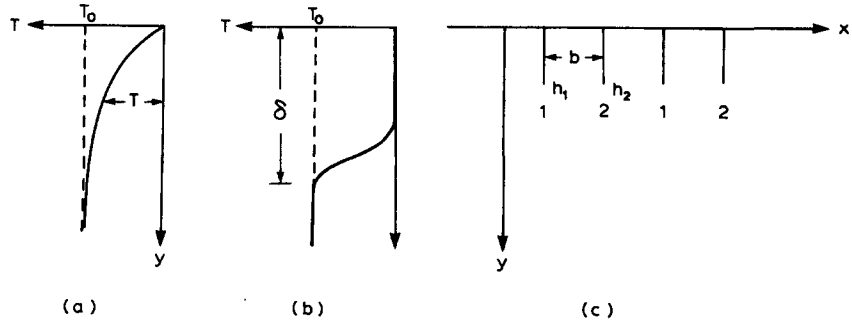

Fig. 1. (a) Temperature profile eqn (2.1); (b) Temperature profile eqn (2.2); (c) Half-plane with equally spaced cracks.

†Permanent address: Department of Mathematics, Indian Institute of Technology, Bombay-400076, India.

An important question is whether these cracks continue to grow or whether some cracks will stop or even close in favor of other cracks, resulting in larger crack spacing; in other words, is the mechanism of equal crack growth a stable process? In the present case the problem is considerably complicated because of the circulation of water through the secondary cracks, which results in a non-uniform temperature distribution in the water. Convective currents are hence set up which in turn, because of the mixing process, change the temperature at the boundary of the solid in the secondary cracks.

In an effort to understand the mechanism and the stability of thermally induced crack growth in brittle elastic solids, we drastically simplify the preceding problem, and consider a homogeneous and isotropic elastic half-space, initially at the uniform temperature T_0, whose free surface is then brought to a temperature T_s (which we set equal to zero), and kept constant thereafter. We shall further assume that the half-space is initially subjected to a uniform compression in one direction parallel to its free surface in such a manner that the cracks are initially formed perpendicular to the free surface (system of parallel cracks), and that the temperature profile in the solid is not altered by the formation and extension of these cracks. Moreover, to simplify the analysis further, we assume that the cracks are equally spaced.

Admittedly this is an oversimplification. However, in view of the lack of information on the stability of crack growth, and because of the accompanying analytical difficulties, we feel that the model will adequately bring into focus some of the delicate and nonconventional considerations which are required for a proper analysis of this class of problems. In fact, because of the existence of a number of constraints, a straightforward application of the well-developed classical elastic stability analysis cannot be made in the present case; for a discussion of elastic stability, see Pearson[2], Hill[3], Nemat-Nasser[4], Thompson and Hunt[5] and Roorda[6]. In Section 2 the basic stability theory for crack growth is developed. In Section 3 the corresponding thermoelasticity problem is formulated in the form of integral equations, and the basic method of solution is outlined. Numerical examples and relevant discussion are then presented in Section 4. Readers who are not interested in the detailed mathematical analysis which is required for the calculation of the stress intensity factors and their derivatives with respect to crack lengths may skip Section 3 and go directly from Section 2 to Section 4.

Finally, it should be noted that the results present in this work have immediate application to the following and related problems:

(1) Cracks formed in thermal shields due to cooling;
(2) Shrinkage cracks in polymers due to aging and loss of moisture;
(3) Shrinkage cracks in adhesively bonded materials, such as paints, polymer films, etc.;
(4) Shrinkage cracks in drying concrete;
(5) Surface cracks in aging wood;
(6) Desiccation cracks in deserts and dried up lakes;
(7) Thermal cracks in nuclear reactor fuel elements, and swelling and thermal cracks in the first wall of some proposed fusion reactor structures;
(8) The growth and interaction of initially star-shaped cracks in hydraulic fracturing.

2. STABILITY ANALYSIS OF CRACK GROWTH

Temperature profiles

Consider a homogeneous isotropic elastic half-space $y \geq 0$. Assume that the initial temperature is uniform and is equal to T_0. Let the surface $y = 0$ be brought to temperature zero and be kept zero thereafter. It is easy to verify that because of heat conduction, the temperature profile in the solid will be given by the following error function (see Fig. 1a):

$$T = T_0 \operatorname{erf}\left(\frac{y\sqrt{3}}{\delta}\right), \qquad y \geq 0, \tag{2.1}$$

where $\operatorname{erf}(x) = (2/\sqrt{\pi}) \int_0^x e^{-u^2} du$; δ is a length scale which increases as the square root of time and can be used as a measure of the depth in which an appreciable temperature gradient has been formed. For the present analysis δ will serve as a "load parameter", which we shall refer to as the "penetration depth".

Simple calculations which ignore the effect of convection heat transfer give the following expression,† $\delta = [tk/\rho C]^{1/2}$. If we use the material constants relevant to granite, for example, we discover that δ increases only a few meters in the span of a year. Therefore, the change in the load parameter, δ, is so slow that a quasi-static analysis is permitted.

As the water moves through the secondary cracks, heat is transferred also by convection. This process tends to cool the rock faster than when no convection takes place. The temperature profile, in this case, will be considerably different from the one shown in Fig. 1(a). A possible profile which may account for the convective effect is sketched in Fig. 1(b). Here it is assumed that the temperature is reduced to zero for a distance equal to $\delta/(n+1)$, and then attains the value T_0 over a distance equal to $n\delta/(n+1)$, so that the total "penetration depth" is still equal to δ. The corresponding temperature field may be approximated by the following:

$$T = 0 \quad \text{for} \quad 0 \leq y \leq \delta/(n+1),$$

$$T = \frac{T_0}{2}\left(1 - \cos \pi \frac{y(n+1) - \delta}{n\delta}\right) \quad \text{for} \quad \delta/(n+1) \leq y \leq \delta \tag{2.2}$$

$$T = T_0 \quad \text{for} \quad \delta \leq y.$$

We shall use for illustration both temperature profiles (2.1) and (2.2). Basically they give similar results. However, they lead to quantitatively different conclusions. We note, however, that neither profile represents the actual case, although they ought to give a reasonable range within which the actual temperature profile may fall.

Statement of problem

We shall assume that the elastic half-space is an ideal brittle material with a constant surface energy γ. Hence, a crack will extend (mode I) in this solid in such a manner that the "stress intensity factor" at the tip of crack does not exceed and remains at the critical value K_c; see, for example, Knott[7]. Since we deal with a plane strain problem, we have

$$K_c = \sqrt{\left(\frac{2\gamma E}{1-\nu^2}\right)}, \tag{2.3}$$

where E is Young's modulus, and ν is Poisson's ratio.

If T_0 is sufficiently large, say 100°C, then after δ attains a suitable value, cracks will form at the surface and penetrate into the half-space. We assume that a uniform compression is (externally) applied normal to the x,y-plane to ensure a state of plane strain even after the formation of cracks. Nevertheless, there is no reason to assume that the initial crack spacing is equal or even periodic. But in order to simplify the required analysis, we shall assume a system of parallel cracks with an initially equal crack spacing b.

As δ increases, the crack length also increases. Excluding crack branching, we shall seek to answer the following basic question:

Would the cracks grow with δ at a common rate, or would some cracks grow faster or even *snap* into a finitely longer length, while the remaining cracks stop growing or even snap closed, when a certain critical state is exceeded?

In other words, is the *equal crack growth regime* a stable process or does this regime change at a certain critical state, after which a different regime prevails? Moreover, if the latter is the case, what exactly is the nature of the new crack growth regime, and to what extent is it affected by the corresponding temperature profile?

In the sequel we shall show that as the cracks grow equally, a critical state may be reached corresponding to a critical value of the load parameter, $\delta = \delta_c$, after which every other crack stops growing, while the remaining cracks grow at a faster rate. This new regime of crack growth will persist until another critical state is reached. At this new critical state, depending on the temperature profile, we may have the following possibilities:

(1) For temperature profile (2.1) the cracks which have stopped growing, together with

†Here k is the conductivity, ρ is the mass-density, C is the heat capacity of the solid, and t measures time.

every other crack of those which had continued to grow, snap closed, while at the same time the remaining cracks snap into a finitely longer length: the crack spacing changes from the initial value b to $4b$ after this state;

(2) For temperature profile (2.2), after the second critical state, on the other hand, only those cracks which had stopped growing snap closed, while all the remaining cracks snap into a slightly longer length: the crack spacing changes from the initial value b to $2b$ after this state.

Stability analysis; non-interacting cracks

We first note that it is the *interaction* between adjacent cracks which leads to the unstable growth modes mentioned above. To show this we proceed as follows.

Assume there are no interactions between adjacent cracks. Then one can consider a "unit cell" of width b consisting of a single crack of length h, as shown in Fig. 2(a). The stress intensity factor is then given by

$$K = K(h; \delta). \tag{2.4}$$

For this crack to grow spontaneously for a *fixed* value of δ, we must have

$$K(h; \delta) = K_c, \quad \mathrm{d}K = \frac{\partial K}{\partial h}\mathrm{d}h > 0 \quad \text{for} \quad \mathrm{d}h > 0,$$

so that we must have $\partial K/\partial h > 0$. Although it is intuitively clear that in the present case this can never happen, we have verified this fact in the following manner: (1) for a given value of δ we have calculated the value of h such that $K = K_c$ (note b is fixed†); (2) for this value of h, we then have calculated $\partial K/\partial h$, which maintains a strictly negative value for all finite values of δ; $\partial K/\partial h$ approaches zero asymptotically as δ goes to infinity. This is shown in Fig. 3, where N is the dimensionless stress intensity factor (see eqn 3.39), $a = h/b$, and $\Delta = \delta/b$.

We therefore see that if the cracks do not interact (when the spacing is very large relative to the common crack length), then the equal crack growth regime is strictly stable.

Stability analysis; interacting cracks

Consider a system of two interacting cracks, as denoted by 1 and 2 in Fig 2(b). Let the corresponding stress intensity factors and lengths be denoted by K_i and h_i, $i = 1, 2$, respectively. Consider the *equilibrium state*

$$h_1 = h_2 = h \quad \text{and} \quad K_1 = K_2 = K_c \tag{2.5}$$

for a given value of δ. As δ increases, h increases such that $K_i = K_c$ is maintained.

We ask: what are the conditions under which such an equilibrium state becomes unstable; moreover, what is the instability *mode*?

To answer these questions, we may either proceed by "the method of adjacent equilibrium state", or we may use a variational approach. In the sequel we shall apply in detail the first

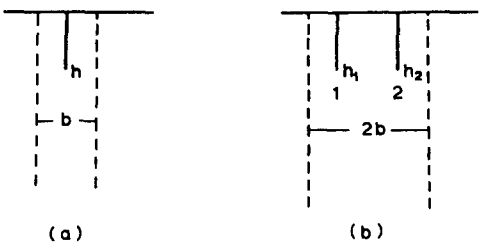

Fig. 2. (a) A typical unit cell with one crack; noninteracting crack system; (b) A typical unit cell with two cracks; interacting crack system.

†For the initial crack spacing, b has calculable minimum values; see Section 4.

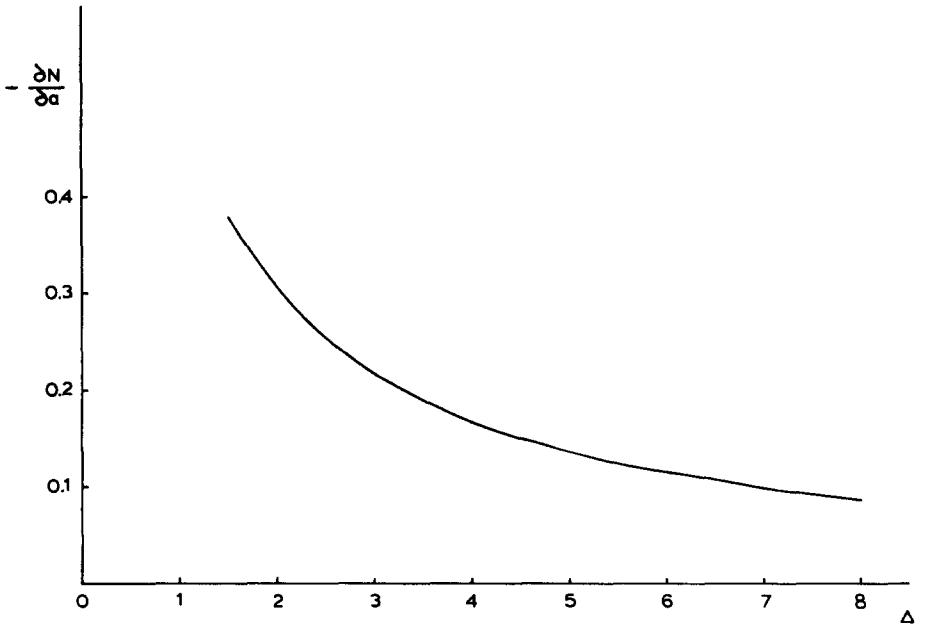

Fig. 3.

method, and then briefly discuss an energy consideration. Both, of course, lead to the same conclusions.

Let the load parameter δ be fixed at δ_0 and consider small changes in the crack lengths. Since $K_i = K_i(h_1, h_2; \delta_0)$, the corresponding changes in the stress intensity factors are given by

$$dK_1 = \frac{\partial K_1}{\partial h_1} dh_1 + \frac{\partial K_1}{\partial h_2} dh_2, \qquad dK_2 = \frac{\partial K_2}{\partial h_1} dh_1 + \frac{\partial K_2}{\partial h_2} dh_2, \tag{2.6}$$

where the partial derivatives are calculated for $\delta = \delta_0$, at the equilibrium state $h_1 = h_2 = h$, where $K_1 = K_2 = K_c$. Hence, if, for example, dK_1 is positive, then crack 1 will grow to a larger length ($dh_1 > 0$) in such a manner that K_1 remains at the critical value K_c. On the other hand, if dK_1 is negative, then K_1 drops below its critical value K_c and therefore crack 1 ceases to grow ($dh_1 = 0$).

Hence, the *admissible* changes in the crack lengths in eqns (2.6) must comply with the following conditions:

$$dh_i \geq 0 \quad \text{for} \quad 0 < K_i \leq K_c. \tag{2.7}$$

In the sequel we shall prove that at the equilibrium state (2.5), we must have

$$\frac{\partial K_1}{\partial h_2} = \frac{\partial K_2}{\partial h_1} < 0 \quad \text{always.} \tag{2.8}$$

With constraints (2.7) and (2.8) it can be immediately concluded from (2.6) that the equilibrium state (2.5) is stable if and only if

$$\frac{\partial K_1}{\partial h_1} = \frac{\partial K_2}{\partial h_2} < 0, \tag{2.9}$$

and that it is unstable if and only if

$$\frac{\partial K_1}{\partial h_1} = \frac{\partial K_2}{\partial h_2} \geq 0, \tag{2.10}$$

where the equality sign defines the critical state.

Conditions (2.9) are sufficient for stability because, in view of (2.7) and (2.8), for any admissible change $dh_i \geq 0$, we have $dK_i \leq 0$, and therefore neither crack can grow spontaneously. These conditions are also necessary because, if they are violated, then one crack (say crack 1) would stop growing ($dh_1 = 0$), and the other crack grow spontaneously ($dh_2 > 0$). As is seen from eqns (2.6), in this case we will have $dK_1 = (\partial K_1/\partial h_2)\, dh_2 < 0$ because of (2.8), and $dK_2 = (\partial K_2/\partial h_2)\, dh_2 > 0$. At the critical state $\partial K_2/\partial h_2 = 0$, and we obtain $dK_1 < 0$ and $dK_2 = 0$, so that $dh_1 = 0$ while $dh_2 > 0$ is undefined. This means the existence of an "adjacent equilibrium state".

Post-critical response

Assume that initially the two cracks are equal and that they grow equally with increasing δ in a stable manner, i.e. conditions (2.9) prevail. Suppose that, for $\delta = \delta_c$ and $h_1 = h_2 = h_c$ conditions (2.9) cease to hold. For $\delta > \delta_c$, one crack, say crack 1, stops growing, remaining at the value $h_1 = h_c$ thereafter, while the other crack continues to grow (possibly at a faster rate) (see Fig. 4). For an increase in δ, we therefore have†

$$dK_1 = \frac{\partial K_1}{\partial h_2} dh_2 + \frac{\partial K_1}{\partial \delta} d\delta < 0, \quad dh_1 = 0$$

$$dK_2 = \frac{\partial K_2}{\partial h_2} dh_2 + \frac{\partial K_2}{\partial \delta} d\delta = 0. \tag{2.11}$$

In this manner, K_1 continues to decrease. The results are schematically shown in Fig. 4. In this figure, P_c corresponds to the critical state at which crack 1 stops growing. On branch P_cP_1, $h_1 = h_c$, $K_1 < K_c$ and $K_2 = K_c$. The states corresponding to this branch are stable as long as $\partial K_2/\partial h_2$ remains negative; note that, although this quantity is zero at point P_c, in general it will be negative at points corresponding to $h_1 = h_c$, but $h_2 > h_c$. It *may happen* that at a certain point P_1, K_1 reduces to zero. This then marks a second critical state. Since the stress intensity factor cannot be negative, then crack 1 may begin to close as δ is increased and as crack 2 extends. This closure is, in general, a dynamic process. What happens (as illustrated in Section 4) is that crack 1 actually snaps closed, while crack 2 attains a finitely longer length, h_2^*, in Fig. 4. On path P_1P^*, K_1 remains zero.

The detailed crack closure process will depend on the nature of the temperature profile. For the examples considered in Section 4, we have been able to prove that when the closure begins, the corresponding crack snaps closed completely. However, it may be possible that for some other examples there would be a partial closure of certain cracks.

From the energy consideration it will be shown below that

$$K_1 \frac{\partial K_1}{\partial h_2} = K_2 \frac{\partial K_2}{\partial h_1}. \tag{2.12}$$

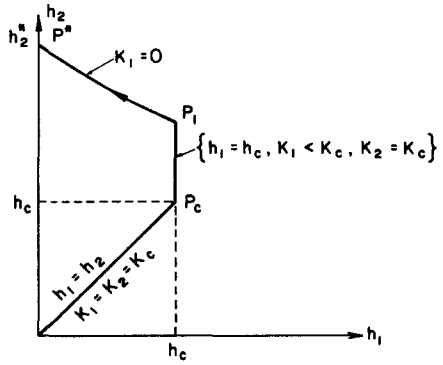

Fig. 4.

†The fact that $dK_1 < 0$ in this regime is a numerical result (see Section 4).

Hence when $K_1 = 0$ and $K_2 = K_c$ (state P_1), we must have

$$\frac{\partial K_2}{\partial h_1} = 0 \tag{2.13}$$

which marks the second critical state.

Energy method

Consider the unit cell of Fig. 2(b) at the equilibrium state (2.5). Let the total elastic energy stored because of nonuniform cooling of the half-plane in the strip of unit thickness (perpendicular to the plane of the paper in Fig. 2b) and of width $2b$ be denoted by $\mathscr{E}$. This energy will be a function of h and δ (among other parameters), i.e. $\mathscr{E} = \mathscr{E}(h, \delta)$. The total surface energy, on the other hand, is $S = 2\gamma(h_1 + h_2) = 4\gamma h$, where γ is the surface energy density. Both $\mathscr{E}$ and S are positive.

Still assuming $h_1 = h_2 = h$, consider for a *fixed* δ an infinitesimal extension of both cracks by an amount Δh. The surface energy then *increases* by $\Delta S = 4\gamma\Delta h > 0$. Since no other source of energy exists (no applied loads), the total elastic energy $\mathscr{E}$ must *decrease* by the amount $\Delta\mathscr{E} = (\partial\mathscr{E}/\partial h)\Delta h < 0$. Thus the energy *release rate* for the crack extension is $-\partial\mathscr{E}/\partial h > 0$.

It is convenient to define $\mathscr{E} = -U$, and to consider the total potential energy of the system of cracks 1 and 2 with lengths h_1 and h_2 in Fig. 2(b), as

$$\Pi = -U + S. \tag{2.14}$$

In this equation $-U$ and S are both positive functions of h_1 and h_2. In accordance with the Griffith crack criterion, the equilibrium state is defined by the vanishing of the first variation of Π, which leads to the equilibrium equations

$$G_i \equiv \frac{\partial U}{\partial h_i} = 2\gamma, \qquad i = 1, 2, \tag{2.15}$$

where G_i is the energy release rate and relates to the stress intensity factor as follows:

$$G_i = \frac{1 - \nu^2}{E} K_i^2. \tag{2.16}$$

Since U is a symmetric function of h_1 and h_2, equilibrium equations (2.15) require that $h_1 = h_2 = h$ at equilibrium.

From (2.15) it is clear that

$$\frac{\partial G_i}{\partial h_j} = \frac{\partial G_j}{\partial h_i}, \tag{2.17}$$

and hence the use of (2.16) in this identity yields (2.12) for unequal cracks.

To study the stability of the equilibrium state (2.5), we consider the second variation of Π, for *admissible* variations of the crack lengths h_1 and h_2. The equilibrium state is stable if the second variation is positive definite, it is critical if the second variation is zero, and it is unstable if the second variation is negative definite. Since the closing of a crack does not result in the retrieval of the corresponding surface energy, admissible variation in h_i must satisfy constraints† (2.7) with $\mathrm{d}h_i = 0$ when $0 < K_i < K_c$, and for $\mathrm{d}h_i < 0$ we must have $K_i = 0$.

The stability conditions are now given by

$$\frac{\partial^2\Pi}{\partial h_i \partial h_j}\,\mathrm{d}h_i\,\mathrm{d}h_j = -\frac{\partial^2 U}{\partial h_i \partial h_j}\,\mathrm{d}h_i\,\mathrm{d}h_j = \begin{cases} > 0 & \text{stable} \\ = 0 & \text{critical, for all } \mathrm{d}h_i \geq 0, \\ < 0 & \text{unstable} \end{cases} \tag{2.18}$$

where repeated indices i and j are summed.

†Note that without these essential restrictions, condition (2.9) *will not be sufficient* for stability. The validity of our results therefore hinges on this fact.

Assume without a loss in generality that $dh_2 > 0$, and set

$$z = dh_1/dh_2, \qquad z \geq 0. \tag{2.19}$$

Then stability conditions (2.18) can be rewritten as

$$F \equiv -\left\{K_1 \frac{\partial K_1}{\partial h_1} z^2 + 2K_2 \frac{\partial K_2}{\partial h_1} z + K_2 \frac{\partial K_2}{\partial h_2}\right\} \begin{cases} > 0 \text{ stable.} \\ = 0 \text{ critical, for all } z \geq 0. \\ < 0 \text{ unstable.} \end{cases} \tag{2.20}$$

In view of (2.8) and (2.19), for $K_1 = K_2 = K_c > 0$, F is strictly positive if and only if (2.9) is satisfied. Moreover, F ceases to be positive, for some z, if (2.10) is satisfied.

Consider now the case when $0 < K_1 < K_c$, $dh_1 = 0$ ($z = 0$), and $K_2 = K_c$; branch P_cP_1 of Fig. 4. Again the corresponding states will be stable as long as $\partial K_2/\partial h_2 < 0$. Figure 5 shows F for different conditions. In this figure we have used the following notation:

$$\alpha = -\partial^2 U/(\partial h_1)^2, \qquad \beta = -\partial^2 U/(\partial h_1 \partial h_2), \qquad \eta = -\partial^2 U/(\partial h_2)^2, \tag{2.21}$$

so that the necessary and sufficient condition for stability of equilibrium state (2.5) now is $\alpha = \eta > 0$; note that in view of (2.8), $\beta > 0$ always. In Fig. 5, we have sketched F as a function of z for $\alpha > 0$ (stable state), $\alpha = 0$ (critical state), and $\alpha < 0$ (unstable state). It is seen that when $\alpha > 0$, F is strictly positive for $z \geq 0$, but it may attain negative values for *inadmissible* values of z, i.e. for $z < 0$. On the other hand, when $\alpha < 0$, F takes on negative values for positive values of z. For $\alpha = 0$, $F = 0$ at $z = 0$, and $F > 0$ for $z > 0$.

Note that if (2.20) were physically meaningful for negative values of z, or if β could take on negative values, then in addition to (2.9), one *must* also require that $\beta^2 - \alpha^2 < 0$ for stability; this is the well-known classical result. *In the present case, however, the sign or the value of the quantity $\beta^2 - \alpha^2$ has no relation whatsoever to the question of stability.* In Fig. 5, curves 1, 2 and 3 are plots of F for *stable regimes* because for these curves $\alpha > 0$. However, for curve 1, $\beta^2 - \alpha^2 < 0$, whereas for all other curves between curves 2 and 4, $\beta^2 - \alpha^2 > 0$; for curve 2, $\beta^2 - \alpha^2 = 0$.

Figure 6 shows the corresponding states in terms of the values of the stress intensity factors K_1 and K_2. In this figure the solid curves are the stress intensity factor for constant values of δ, and for $h_1 = h_2$. The fundamental equilibrium path corresponds to the intersection of these curves with the horizontal line $K_1 = K_2 = K_c$. Suppose we consider the state A on the equilibrium path. Since $\alpha > 0$ at A, this state is stable. As δ is increased, this point moves to the left parallel to the horizontal axis, and the corresponding equilibrium states are stable, as long as the variation of K_1 with respect to h_1, or K_2 with respect to h_2, for the corresponding constant value of δ, is negative, i.e. as long as $\alpha > 0$. At point B, $\alpha = 0$, and therefore $\partial K_2/\partial h_2 = 0$. This

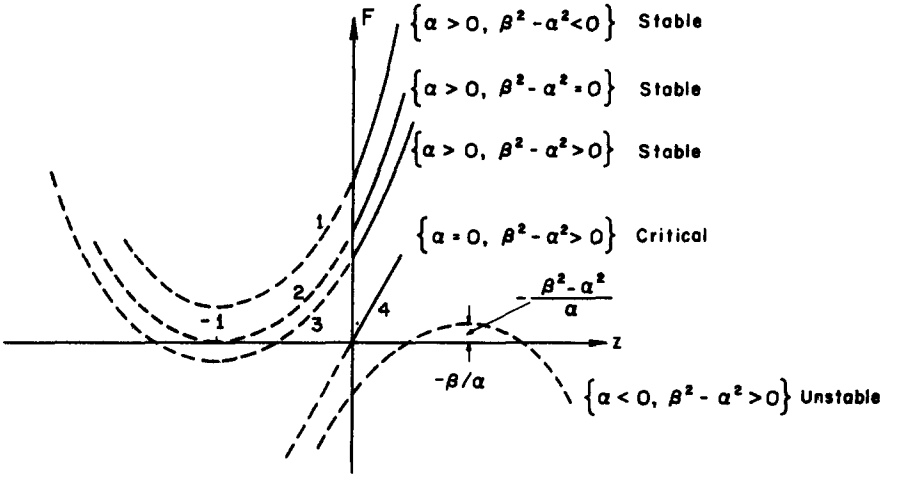

Fig. 5. Second variation of potential energy as a function of $z = dh_1/dh_2$.

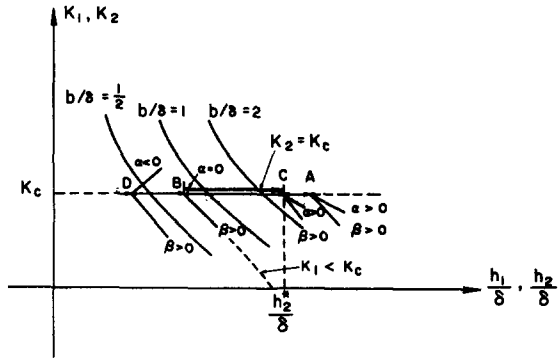

Fig. 6.

point corresponds to the critical state. A snap-through can then occur which results in a new crack length for crack 2 given by the abscissa of point C. The stress intensity factor at crack 1 first decreases, falling below K_c, which means that crack 1 stops growing. If and when the stress intensity at crack 1 reaches zero value, before state C is attained, then crack 1 begins to close.

Additional comments

The interaction between the two cracks as they grow may be better understood if one replaces the effect of nonuniform cooling, by *equivalent* surface tractions and body forces. Except for an insignificant equivalent body force, as far as the values of the stress intensity factors are concerned the effect of cooling can be represented by equivalent distributed normal tractions on the faces of the crack, as shown in Fig. 7(a); see also eqns (3.1) of Section 3. First, note, e.g. for temperature profile (2.1), that when δ is very small, the equivalent normal tractions τ_{xx} at $x = 0, b$, decrease very quickly with respect to increasing y. On the other hand, this decrease becomes much more gradual as δ increases.

Consider now a small increase in h_2 for fixed values of δ and h_1; see Fig. 7(b). The corresponding compressive forces on the faces of crack 2 increase by the amount ΔF, which tend to decrease the tensile stress τ_{xx}, at the vicinity of crack 1, i.e. $\partial K_1/\partial h_2$ must be negative, as stated before; see eqn (2.8).

Consider now the change in the stress field around crack 2, when δ and h_1 are held fixed, and h_2 is increased by a small amount. The corresponding increase, ΔF, in the total compressive forces tends to *increase* the stress intensity factor K_2. On the other hand, if ΔF were zero, the increase in h_2 would *decrease* K_2. When δ is small, then ΔF will be small, and hence the decrease in K_2 because of the increase in h_2 is larger than the corresponding increase in K_2 because of the addition of the compressive forces ΔF. Hence, for suitably small values of δ, we must have $\partial K_2/\partial h_2 < 0$. As δ increases, ΔF becomes more dominant. At a critical value δ_c of δ, the two effects cancel each other, and we have the critical condition $\partial K_2/\partial h_2 = 0$.

Since the two cracks are completely symmetrical, they are initially equal and grow at an equal rate, while $\partial K_2/\partial h_2 = \partial K_1/\partial h_1 < 0$; i.e. stable growth. At the critical state, equal

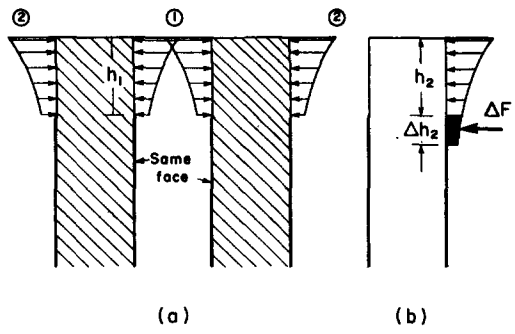

Fig. 7. Two interacting cracks subjected to equivalent surface tractions.

continuous crack growth becomes impossible, since it leads to the state with $\partial K_2/\partial h_2 = \partial K_1/\partial h_1 > 0$. At this state, one crack stops growing and the other crack grows faster with increasing δ, while maintaining $\partial K_2/\partial h_2 < 0$ and $K_1 < K_c$ (nonsymmetric instability mode). Our calculations for the examples in Section 4 have shown that this is the instability mode which occurs in this case. Moreover, that not only does every other crack stop growing after the critical state, but also that these cracks may actually snap closed after a second critical state is reached.† Note that every other crack closes and the corresponding displacement jumps vanish; *there is no interpenetration of matter involved in this crack closure process.*

3. ANALYSIS

We shall now formulate the plane problem of a half-space weakened by a system of equally space parallel cracks with alternate lengths h_1 and h_2. Let the spacing be b, and let the cracks be opened by a nonuniform temperature distribution (cooling) given by either eqn (2.1) or eqn (2.2). The problem is equivalent to that in which the cracks are subject to the applied stresses given by

$$\begin{cases} \tau_{xx}(0, y) = -\hat{\beta} T_0 f(y/\delta), \\ \tau_{xy}(0, y) = 0, \quad \text{for } 0 < y < h_1, \end{cases} \qquad \begin{cases} \tau_{xx}(b, y) = -\hat{\beta} T_0 f(y/\delta), \\ \tau_{xy}(b, y) = 0, \quad \text{for } 0 < y < h_2, \end{cases} \tag{3.1}$$

where $\hat{\beta} = 3\hat{\alpha}E/(1-2\nu)$, $\hat{\alpha}$ being the coefficient of thermal expansion, and where $f(y/\delta)$ represents the corresponding profile for temperature distribution.

Basic equations

A suitable representation for the components of stress for a vertical crack below an elastic half-space is given by Keer and Chantaramungkorn[8]. This form can be modified to account for an array of cracks with the stresses on the crack faces written as follows:

$$\tau_{xx}(0, y) = \int_0^{h_1} D_1(t) \sum_{n=-\infty}^{\infty} G(t, 2nb, y)\, dt + \int_0^{h_2} D_2(t) \sum_{N=-\infty}^{\infty} G(t, b + 2nb, y)\, dt, \tag{3.2}$$

and

$$\tau_{xx}(b, y) = \int_0^{h_1} D_1(t) \sum_{n=-\infty}^{\infty} G(t, b + 2nb, y)\, dt + \int_0^{h_2} D_2(t) \sum_{n=-\infty}^{\infty} G(t, 2nb, y)\, dt. \tag{3.3}$$

The functions $D_1(t), D_2(t)$ represent dislocation densities and because of symmetry on $x = 0, b$, the shear stress terms have been omitted; the kernel G is given by

$$G(t, x, y) = \frac{2(y+t)}{(y+t)^2 + x^2} - \frac{(y+3t)[(y+t)^2 - x^2]}{[(y+t)^2 + x^2]^2} + \frac{4ty(y+t)[(y+t)^2 - 3x^2]}{[(y+t)^2 + x^2]^3} - \frac{(y-t)[(y-t)^2 + 3x^2]}{[(y-t)^2 + x^2]^2}. \tag{3.4}$$

Since G is an even function of x, the series in (3.2) and (3.3) may be written as

$$\sum_{n=-\infty}^{\infty} G(t, 2nb, y) = G(t, 0, y) + 2 \sum_{n=1}^{\infty} G(t, 2nb, y), \tag{3.5}$$

$$\sum_{n=-\infty}^{\infty} G(t, b + 2nb, y) = 2 \sum_{n=1}^{\infty} G(t, (2n-1)b, y). \tag{3.6}$$

Fortunately, the above series can be summed in closed form. Indeed, if we make use of the

†In terms of Fig. 7(b), this means that, at the second critical state, the "equivalent" normal tractions on the longer crack 2 may now overcome the tractions which are keeping crack 1 open. A further increase in crack 2 leads to larger equivalent tractions which then overcome tractions on crack 1; crack 1 closes as crack 2 extends (instability).

formulae, see Gradshteyn and Ryzhik ([9], pp. 23, p. 36),

$$\sum_{n=1}^{\infty} \frac{1}{x^2+n^2} = \frac{1}{2x^2}[\pi x \coth \pi x - 1], \tag{3.7}$$

$$\sum_{n=1}^{\infty} \frac{1}{x^2+(2n-1)^2} = \frac{\pi}{4x} \tanh \frac{\pi x}{2}, \tag{3.8}$$

we can write

$$\begin{aligned} 2\sum_{n=1}^{\infty} G(t, 2nb, y) = {} & \frac{t^2-y^2-4ty}{(y+t)^3} + \frac{\pi}{b}\coth\frac{\pi(y+t)}{2b} - \frac{(y+3t)\pi^2}{4b^2}\operatorname{cosech}^2\frac{\pi(y+t)}{2b} \\ & + \frac{ty\pi^3}{2b^3}\operatorname{cosech}^2\frac{\pi(y+t)}{2b}\coth\frac{\pi(y+t)}{2b} \\ & + \frac{1}{(y-t)}\left[1 - \frac{\pi(y-t)}{b}\coth\frac{\pi(y-t)}{2b} \right. \\ & \left. + \frac{\pi^2(y-t)^2}{4b^2}\operatorname{cosech}^2\frac{\pi(y-t)}{2b}\right], \end{aligned} \tag{3.9}$$

$$\begin{aligned} 2\sum_{n=1}^{\infty} G(t, (2n-1)b, y) = {} & \frac{\pi}{b}\tanh\frac{\pi(y+t)}{2b} + \frac{(y+3t)\pi^2}{4b^2}\operatorname{sech}^2\frac{\pi(y+t)}{2b} \\ & - \frac{\pi^3 ty}{2b^3}\operatorname{sech}^2\frac{\pi(y+t)}{2b}\tanh\frac{\pi(y+t)}{2b} \\ & - \frac{\pi}{4b}\left[4\tanh\frac{\pi(y-t)}{2b} + \frac{\pi(y-t)}{b}\operatorname{sech}^2\frac{\pi(y-t)}{2b}\right]. \end{aligned} \tag{3.10}$$

Also, from (3.4) we have

$$G(t, 0, y) = \frac{1}{t-y} - \frac{t^2-y^2-4ty}{(y+t)^3}. \tag{3.11}$$

The unknown functions D_1, D_2 in (3.2) and (3.3) are to be determined by the boundary conditions (3.1). Setting †

$$D_1(t) = \left(\frac{h_1}{h_1^2-t^2}\right)^{1/2} C_1(t), \qquad D_2(t) = \left(\frac{h_2}{h_2^2-t^2}\right)^{1/2} C_2(t), \tag{3.12}$$

$$G(t, 0, y) + 2\sum_{n=1}^{\infty} G(t, 2nb, y) = \frac{\pi}{2b} G_1\left(\frac{\pi t}{2b}, \frac{\pi y}{2b}\right), \tag{3.13}$$

$$2\sum_{n=1}^{\infty} G(t, (2n-1)b, y) = \frac{\pi}{2b} G_2\left(\frac{\pi t}{2b}, \frac{\pi y}{2b}\right), \tag{3.14}$$

and making use of the relations (3.1)–(3.3), (3.5), (3.6) and (3.9)–(3.11), we get

$$\frac{\pi}{2b}\int_0^{h_1} C_1(t)\left(\frac{h_1}{h_1^2-t^2}\right)^{1/2} G_1\left(\frac{\pi t}{2b}, \frac{\pi y}{2b}\right) dt + \frac{\pi}{2b}\int_0^{h_2} C_2(t)\left(\frac{h_2}{h_2^2-t^2}\right)^{1/2} G_2\left(\frac{\pi t}{2b}, \frac{\pi y}{2b}\right) dt = -\hat{\beta} T_0 f(y/\delta), \quad 0 < y < h_1, \tag{3.15}$$

$$\frac{\pi}{2b}\int_0^{h_1} C_1(t)\left(\frac{h_1}{h_1^2-t^2}\right)^{1/2} G_2\left(\frac{\pi t}{2b}, \frac{\pi y}{2b}\right) dt + \frac{\pi}{2b}\int_0^{h_2} C_2(t)\left(\frac{h_2}{h_2^2-t^2}\right)^{1/2} G_1\left(\frac{\pi t}{2b}, \frac{\pi y}{2b}\right) dt = -\hat{\beta} T_0 f(y/\delta), \quad 0 < y < h_2, \tag{3.16}$$

†These equations exhibit the singularities of $D_1(t)$, $D_2(t)$ at the crack ends; note that $D_1(t)$ and $D_2(t)$ do not have singularities at $t = 0$.

where G_1, G_2 are given by

$$G_1(t, y) = \frac{1}{t-y} + 2\coth(y+t) - (y+3t)\operatorname{cosech}^2(y+t) + 4ty\operatorname{cosech}^2(y+t)\coth(y+t)$$
$$+ \frac{1}{y-t}[1 - 2(y-t)\coth(y-t) + (y-t)^2\operatorname{cosech}^2(y-t)], \tag{3.17}$$

$$G_2(t, y) = 4t + 2\tanh(y+t) - (y+3t)\tanh^2(y+t) - 4ty\tanh(y+t)\{1 - \tanh^2(y+t)\}$$
$$- 2\tanh(y-t) + (y-t)\tanh^2(y-t). \tag{3.18}$$

We note that, except for the first term in G_1, both of the functions G_1 and G_2 are bounded in the rectangles of their definitions. Since D_1, D_2 are proportional to the stresses on the lines of the cracks, the new unknown functions in the integral eqns (3.15) and (3.16) are also bounded functions on the intervals of their definitions.

Let k_1, k_2 denote† the stress intensity factors at the crack tips $(0, h_1)$ and (b, h_2), respectively, then using (3.2), (3.5), (3.12), (3.13) and (3.17) we have

$$k_1 = \lim_{y\to h_1^+} \sqrt{(y-h_1)}\,\tau_{xx}(0, y) = \lim_{y\to h_1^+} \sqrt{(y-h_1)} \int_0^{h_1} C_1(t)\left(\frac{h_1}{h_1 - t}\right)^{1/2} \frac{dt}{t-y}$$
$$= \lim_{y\to h_1^+} \sqrt{(y-h_1)}\, h_1 \int_0^{h_1} \frac{C_1(y) + \{C_1(t) - C_1(y)\}}{(t-y)\sqrt{(h_1^2 - t^2)}}\, dt, \tag{3.19}$$

or

$$k_1 = \lim_{y\to h_1^+} \sqrt{(y-h_1)}\, h_1 C_1(y)\left\{\frac{-i\pi}{\sqrt{(h_1^2 - y^2)}}\right\} = -\pi\sqrt{(h_1/2)}\, C_1(h_1). \tag{3.20}$$

Similarly, using (3.3), (3.6), (3.12), (3.14) and (3.18), we can show that

$$k_2 = -\pi\sqrt{(h_2/2)}\, C_2(h_2). \tag{3.21}$$

Numerical method

To solve integral equations (3.15) and (3.16) numerically, we first normalize the intervals $(0, h_1)$ and $(0, h_2)$ by defining

$$s = t/h_1, \quad x = y/h_1 \quad \text{for} \quad 0 < t, \quad y < h_1,$$
$$s = t/h_2, \quad x = y/h_2 \quad \text{for} \quad 0 < t, \quad y < h_2,$$

and by setting

$$C_1(h_1 s) = B_1(s) \quad \text{and} \quad C_2(h_2 s) = B_2(s). \tag{3.22}$$

We can now write singular integral equations (3.15) and (3.16) in the form

$$\frac{\pi h_1}{2b}\int_0^1 \frac{B_1(s)}{(1-s^2)^{1/2}} G_1\left(\frac{\pi h_1 s}{2b}, \frac{\pi h_1 x}{2b}\right) ds + \frac{\pi h_2}{2b}\int_0^1 \frac{B_2(s)}{(1-s^2)^{1/2}} G_2\left(\frac{\pi h_2 s}{2b}, \frac{\pi h_2 x}{2b}\right) ds$$
$$= -\hat{\beta} T_0 f(h_1 x/\delta), \qquad 0 < x < 1, \tag{3.23}$$

$$\frac{\pi h_1}{2b}\int_0^1 \frac{B_1(s)}{(1-s^2)^{1/2}} G_2\left(\frac{\pi h_1 s}{2b}, \frac{\pi h_2 x}{2b}\right) ds + \frac{\pi h_2}{2b}\int_0^1 \frac{B_2(s)}{(1-s^2)^{1/2}} G_1\left(\frac{\pi h_2 s}{2b}, \frac{\pi h_2 x}{2b}\right) ds$$
$$= -\hat{\beta} T_0 f(h_2 x/\delta), \qquad 0 < x < 1. \tag{3.24}$$

A practical technique for solving (3.23) and (3.24) is obtained if we extend functions $B_1(s)$

†According to the definition used in Section 2, $k_i = K_i/\sqrt{(2\pi)}$, $i = 1, 2$

and $B_2(s)$ into the interval $(-1, 0)$. An appropriate extension of this kind is the following even continuation:

$$B_1(-s) = B_1(s), \quad B_2(-s) = B_2(s), \quad -1 < s < 1. \tag{3.25}$$

With the aid of (3.25) we can write (3.23) and (3.24) in the form

$$\frac{1}{2}\int_{-1}^{1} \frac{B_1(s)}{(1-s^2)^{1/2}} \frac{\pi h_1}{2b} G_1\left(\left|\frac{\pi h_1 s}{2b}\right|, \frac{\pi h_1 x}{2b}\right) ds + \frac{1}{2}\int_{-1}^{1} \frac{B_2(s)}{(1-s^2)^{1/2}} \frac{\pi h_2}{2b} \times G_2\left(\left|\frac{\pi h_2 s}{2b}\right|, \frac{\pi h_1 x}{2b}\right) ds = -\hat{\beta} T_0 f(h_1 x/\delta), \quad 0 < x < 1, \tag{3.26}$$

$$\frac{1}{2}\int_{-1}^{1} \frac{B_1(s)}{(1-s^2)^{1/2}} \frac{\pi h_1}{2b} G_2\left(\left|\frac{\pi h_1 s}{2b}\right|, \frac{\pi h_2 x}{2b}\right) ds + \frac{1}{2}\int_{-1}^{1} \frac{B_2(s)}{(1-s^2)^{1/2}} \frac{\pi h_2}{2b} \times G_1\left(\left|\frac{\pi h_2 s}{2b}\right|, \frac{\pi h_2 x}{2b}\right) ds = -\hat{\beta} T_0 f(h_2 x/\delta), \quad 0 < x < 1. \tag{3.27}$$

We now use the integration formula corresponding to the weight function $(1-s^2)^{-1/2}$, as described by Erdogan, Gupta and Cook[10], observe that $s = 0$ is a zero of $G_1(s, x)$ and $G_2(s, x)$, and we obtain

$$-\hat{\beta} T_0 f(h_1 x_k/\delta) = \frac{1}{2}\sum_{i=1}^{2n_1+1} \frac{\pi}{2n_1+1} B_1(s_i) \frac{\pi h_1}{2b} G_1\left(\left|\frac{\pi h_1 s_i}{2b}\right|, \frac{\pi h_1 x_k}{2b}\right) + \frac{1}{2}\sum_{j=1}^{2n_2+1} \frac{\pi}{2n_2+1} B_2(s_j) \frac{\pi h_2}{2b} \times G_2\left(\left|\frac{\pi h_2 s_j}{2b}\right|, \frac{\pi h_1 x_k}{2b}\right), \quad k = 1, 2, \ldots, n_1$$

$$= \sum_{i=1}^{n_1} \frac{\pi}{2n_1+1} B_1(s_i) \frac{\pi h_1}{2b} G_1\left(\frac{\pi h_1 s_i}{2b}, \frac{\pi h_1 x_k}{2b}\right) + \sum_{j=1}^{n_2} \frac{\pi}{2n_2+1} B_2(s_j) \frac{\pi h_2}{2b} \times G_2\left(\frac{\pi h_2 s_j}{2b}, \frac{\pi h_1 x_k}{2b}\right), \quad k = 1, 2, \ldots, n_1, \tag{3.28}$$

$$-\hat{\beta} T_0 f(h_2 x_l/\delta) = \sum_{i=1}^{n_1} \frac{\pi}{2n_1+1} B_1(s_i) \frac{\pi h_1}{2b} G_2\left(\frac{\pi h_1 s_i}{2b}, \frac{\pi h_2 x_l}{2b}\right) + \sum_{j=1}^{n_2} \frac{\pi}{2n_2+1} B_2(s_j) \frac{\pi h_2}{2B} G_1\left(\frac{\pi h_2 s_j}{2b}, \frac{\pi h_2 x_l}{2b}\right), \quad l = 1, 2, \ldots, n_2, \tag{3.29}$$

where

$$s_i = \cos\left(\frac{2i-1}{4n_1+2}\pi\right), \quad x_k = \cos\left(\frac{k\pi}{2n_1+1}\right),$$

$$s_j = \cos\left(\frac{2j-1}{4n_2+2}\pi\right), \quad x_l = \cos\left(\frac{l\pi}{2n_2+1}\right). \tag{3.30}$$

Let

$$a_1 = \frac{h_1}{b}, \quad a_2 = \frac{h_2}{b}, \quad \Delta = \frac{\delta}{b},$$

$$t_{1i} = \frac{\pi a_1}{2} s_i, \quad t_{2j} = \frac{\pi a_2}{2} s_j, \tag{3.31}$$

$$y_{1k} \frac{\pi a_1}{2} x_k, \quad y_{2l} = \frac{\pi a_2}{2} x_l,$$

then eqns (3.28) and (3.29) may be written as

$$\sum_{i=1}^{n_1} \frac{\pi}{(2n_1+1)} B_1(s_i) H_1(t_{1i}, y_{1k}; a_1) + \sum_{j=1}^{n_2} \frac{\pi}{(2n_2+1)} B_2(s_j) H_2(t_{2j}, y_{1k}; a_2) = -\hat{\beta} T_0 f\left(\left(\frac{2}{\pi\Delta} y_{1k}\right)\right), \quad k = 1, 2, \ldots, n_1, \tag{3.32}$$

$$\sum_{i=1}^{n_1} \frac{\pi}{(2n_1+1)} B_1(s_i) H_2(t_{1i}, y_{2l}; a_1) + \sum_{j=1}^{n_2} \frac{\pi}{(2n_2+1)} B_2(s_j) H_1(t_{2j}, y_{2l}; a_2) = -\hat{\beta} T_0 f\left(\frac{2}{\pi\Delta} y_{2l}\right), \quad l = 1, 2, \ldots, n_2, \tag{3.33}$$

where

$$H_1(t, y; a) = \frac{\pi a}{2}\{4t + 2\coth(y+t) - (y+3t)\coth^2(y+t) - 4ty\coth(y+t)[1-\coth^2(y-t)] - 2\coth(y-t) + (y-t)\coth^2(y-t)\}, \tag{3.34}$$

$$H_2(t, y; a) = \frac{\pi a}{2}\{4t + 2\tanh(y+t) - (y+3t)\tanh^2(y+t) - 4ty\tanh(y+t)[1-\tanh^2(y-t)] - 2\tanh(y-t) + (y-t)\tanh^2(y-t)\}. \tag{3.35}$$

If we introduce

$$A_1(s_i) = -\frac{\pi}{2n_1+1}\frac{1}{\hat{\beta}T_0} B_1(s_i), \qquad i = 1, \ldots, n_1,$$

$$A_2(s_j) = -\frac{\pi}{2n_2+1}\frac{1}{\hat{\beta}T_0} B_2(s_j), \qquad j = 1, \ldots, n_2, \tag{3.36}$$

then (3.32) and (3.33) become

$$\sum_{i=1}^{n_1} A_1(s_i) H_1(t_{1i}, y_{1k}; a_1) + \sum_{j=1}^{n_2} A_2(s_j) H_2(t_{2j}, y_{1k}; a_2) = f\left(\frac{2}{\pi\Delta} y_{1k}\right), \quad k = 1, 2, \ldots, n_1, \tag{3.37}$$

$$\sum_{i=1}^{n_1} A_1(s_i) H_2(t_{1i}, y_{2l}; a_1) + \sum_{j=1}^{n_2} A_2(s_j) H_1(t_{2j}, y_{2l}; a_2) = f\left(\frac{2}{\pi\Delta} y_{2l}\right), \quad l = 1, 2, \ldots, n_2. \tag{3.38}$$

Let us define the nondimensional stress intensity factors N_1 and N_2 at the crack tips $(0, h_1)$ and (b, h_2), respectively, by

$$N_1 = \frac{k_1}{\hat{\beta}T_0\sqrt{b}}, \qquad N_2 = \frac{k_2}{\hat{\beta}T_0\sqrt{b}}. \tag{3.39}$$

Then using (3.20), (3.21), (3.22) and (3.36) we have

$$N_1 = (2n_1+1)\sqrt{\left(\frac{a_1}{2}\right)} A_1(1), \qquad N_2 = (2n_2+1)\sqrt{\left(\frac{a_2}{2}\right)} A_2(1). \tag{3.40}$$

We now employ the approximate polynomial solution, as described by Krenk[11], and obtain

$$A_1(1) = \frac{2}{2n_1+1}\left\{\sum_{i=1}^{n_1} (-1)^{i+1} \operatorname{cosec}\left(\frac{2i-1}{4n_1+2}\pi\right) A_1(s_i) + \frac{(-1)^{n_1}}{2} A_1(0)\right\}, \tag{3.41}$$

$$A_2(1) = \frac{2}{2n_2+1}\left\{\sum_{j=1}^{n_2} (-1)^{j+1} \operatorname{cosec}\left(\frac{2j-1}{4n_2+2}\pi\right) A_2(s_j) + \frac{(-1)^{n_1}}{2} A_2(0)\right\}. \tag{3.42}$$

Hence, N_1, N_2 can be written in the form

$$N_1 = \sqrt{(2a_1)}\left\{\sum_{i=1}^{n_1} (-1)^{i+1} \operatorname{cosec}\left(\frac{2i-1}{4n_1+2}\pi\right) A_1(s_i) + \frac{(-1)^{n_2}}{2} A_1(0)\right\}, \tag{3.43}$$

$$N_2 = \sqrt{(2a_2)}\left\{\sum_{j=1}^{n_2} (-1)^{j+1} \operatorname{cosec}\left(\frac{2j-1}{4n_2+2}\pi\right) A_2(s_j) + \frac{(-1)^{n_2}}{2} A_2(0)\right\}, \tag{3.44}$$

where $A_1(0)$, $A_2(0)$ are obtained by interpolation.

The derivatives of the stress intensity factors N_1, N_2 with respect to a_1, using (3.43) and (3.44), are given by

$$\frac{\partial N_1}{\partial a_1}=\frac{N_i}{2a_1}+\sqrt{(2a_1)}\left\{\sum_{i=1}^{n_1}(-1)^{i+1}\operatorname{cosec}\left(\frac{2i-1}{4n_1+2}\pi\right)\frac{\partial}{\partial a_1}A_1(s_i)+\frac{(-1)^{n_1}}{2}\frac{\partial A_1(0)}{\partial a_1}\right\}, \tag{3.45}$$

$$\frac{\partial N_2}{\partial a_1}=\sqrt{(2a_2)}\left\{\sum_{j=1}^{n_2}(-1)^{j+1}\operatorname{cosec}\left(\frac{2j-1}{4n_2+2}\pi\right)\frac{\partial}{\partial a_1}A_2(s_j)+\frac{(-1)^{n_2}}{2}\frac{\partial A_2(0)}{\partial a_1}\right\}. \tag{3.46}$$

where $(\partial/\partial a_1)A_1(s_i)$ and $(\partial/\partial a_1)A_2(s_j)$, $(s_i, s_j\neq 0)$ are found from (3.37) and (3.38) which may be written as

$$\begin{aligned}&\sum_{i=1}^{n_1}\frac{\partial}{\partial a_1}A_1(s_i)H_1(t_{1i}, y_{1k}; a_1)+\sum_{j=1}^{n_2}\frac{\partial}{\partial a_1}A_2(s_j)H_2(t_{2j}, y_{1k}; a_2)\\&\quad=\frac{\partial}{\partial a_1}f\left(\frac{2}{\pi\Delta}y_{1k}\right)-\sum_{i=1}^{n_1}A_1(s_i)\frac{\partial}{\partial a_1}H_1(t_{1i}, y_{1k}; a_1)\\&\quad-\sum_{j=1}^{n_2}A_2(s_j)\frac{\partial}{\partial a_1}H_2(t_{2j}, y_{1k}; a_2), \qquad k=1,\ldots,n_1,\end{aligned} \tag{3.47}$$

$$\begin{aligned}&\sum_{i=1}^{n_1}\frac{\partial}{\partial a_1}A_1(s_i)H_2(t_{1i}, y_{2k}; a_1)+\sum_{j=1}^{n_2}\frac{\partial}{\partial a_1}A_2(s_j)H_1(t_{2j}, y_{2l}; a_2)\\&\quad=-\sum_{i=1}^{n_1}A_1(s_i)\frac{\partial}{\partial a_1}H_2(t_{1i}, y_{2l}), \qquad l=1,\ldots,n_2.\end{aligned} \tag{3.48}$$

The values of $\partial A_1(s_i)/\partial a_1$, $\partial A_2(s_j)/\partial a_1$ at $s_i=s_j=0$ are obtained by interpolation. If we set

$$L_1(xt, xy)=\frac{\partial}{\partial x}H_1(xt, xy; x), \tag{3.49}$$

$$L_2(xt, zy)=\frac{\partial}{\partial x}H_2(xt, zy; x), \tag{3.50}$$

$$L_3(xt, zy)=\frac{z}{x}\frac{\partial}{\partial z}H_2(xt, zy; x), \tag{3.51}$$

then using (3.34) and (3.35) we arrive at

$$\begin{aligned}L_1(t, y)=\frac{\pi}{2}\{&12t+2\coth(y+t)-4(y+2t)\coth^2(y+t)\\&+2(y^2+10ty+3t^2)\coth(y+t)[\coth^2(y+t)-1]\\&-4ty(y+t)[\coth^2(y+t)-1][3\coth^2(y+t)-1]-2\coth(y-t)+4(y-t)\coth^2(y-t)\\&-2(y-t)^2\coth(y-t)[\coth^2(y-t)-1]\},\end{aligned} \tag{3.52}$$

$$\begin{aligned}L_2(t, y)=\frac{\pi}{2}\{&12t+2\tanh(y+t)-(y+8t)\tanh^2(y+t)-2t(5y+3t)\tanh(y+t)[1-\tanh^2(y+t)]\\&-4t^2y[1-\tanh^2(y+t)][1-3\tanh^2(y+t)]-2\tanh(y-t)+(y-4t)\tanh^2(y-t)\\&-2t(y-t)\tanh(y-t)[1-\tanh^2(y-t)]\},\end{aligned} \tag{3.53}$$

$$\begin{aligned}L_3(t, y)=\frac{\pi}{2}\{&-3y\tanh^2(y+t)-2y(y+5t)\tanh(y+t)[1-\tanh^2(y+t)]-4ty^2[1-\tanh^2(y+t)]\\&\times[1-3\tanh^2(y+t)]+3y\tanh^2(y-t)+2y(y-t)\tanh(y-t)[1-\tanh^2(y-t)]\}.\end{aligned} \tag{3.54}$$

For the temperature profile given by (2.1), we use the definition of the error function, and write the first term on the right-hand side of (3.47) as

$$\frac{\partial}{\partial a_1}f\left(\frac{2}{\pi\Delta}y_{1k}\right)=-\frac{2}{a_1\sqrt{\pi}}\left(\frac{2\sqrt{3}}{\pi\Delta}y_{1k}\right)\exp\left[-\left(\frac{2\sqrt{3}}{\pi\Delta}y_{1k}\right)^2\right]. \tag{3.55}$$

In a similar manner, we obtain for temperature profile (2.2),

$$\frac{\partial}{\partial a_1} f\left(\frac{2}{\pi\Delta} y_{1k}\right) = 0, \qquad 0 < \frac{2y_{1k}}{\pi\Delta} < \frac{1}{n+1} = -\frac{(n+1)y_{1k}}{n\Delta a_1} \sin\left[\frac{\pi}{n}\left(\frac{2y_{1k}(n+1)}{\pi\Delta} - 1\right)\right],$$

$$\frac{1}{n+1} < \frac{2y_{1k}}{\pi\Delta} < 1. \tag{3.56}$$

Making use of the relations (3.49) to (3.55) we can write eqns (3.47) and (3.48) in the form

$$\sum_{i=1}^{n_1} \frac{\partial}{\partial a_1} A_1(s_i) H_1(t_{1i}, y_{1k}; a_1) + \sum_{j=1}^{n_2} \frac{\partial}{\partial a_1} A_2(s_j) H_2(t_{2j}, y_{1k}; a_2)$$

$$= -\frac{2}{a_1\sqrt{\pi}}\left(\frac{2\sqrt{3}}{\pi\Delta} y_{1k}\right) \exp\left[-\left(\frac{2\sqrt{3}}{\pi\Delta} y_{1k}\right)^2\right] - \sum_{i=1}^{n_1} A_1(s_i) L_1(t_{1i}, y_{1k})$$

$$- \frac{a_2}{a_1} \sum_{j=1}^{n_2} A_2(s_j) L_3(t_{2j}, y_{1k}), \quad k = 1, \ldots, n_1, \tag{3.57}$$

$$\sum_{i=1}^{n_1} \frac{\partial}{\partial a_1} A_1(s_i) H_2(t_{1i}, y_{2l}; a_1) + \sum_{j=1}^{n_2} \frac{\partial}{\partial a_1} A_2(s_j) H_1(t_{2j}, y_{2l}; a_2)$$

$$= -\sum_{i=1}^{n_1} A_1(s_i) L_2(t_{1i}, y_{2l}), \qquad l = 1, \ldots, n_2; \tag{3.58}$$

for the temperature profile given by (2.2), the corresponding terms in eqns (3.57) must be replaced by the expression (3.56). Since $A_1(s_i)$ and $A_2(s_j)$ can be determined from eqns (3.37) and (3.38), the right-hand sides of the above equations are known. Once $(\partial/\partial a_1)A_1(s_i)$ and $(\partial/\partial a_1)A_2(s_j)$ are obtained by solving (3.57) and (3.58), the derivatives with respect to a_1 of the stress intensity factors N_1, N_2 are given by eqns (3.45) and (3.46).

Similarly, using (3.37) to (3.44), we can show that the derivatives of N_1, N_2 with respect to a_2 are given by

$$\frac{\partial N_1}{\partial a_2} = \sqrt{(2a_1)}\left\{\sum_{i=1}^{n_1} (-1)^{i+1} \operatorname{cosec}\left(\frac{2i-1}{4n_1+2}\pi\right) \frac{\partial}{\partial a_2} A_1(s_i) + \frac{(-1)^{n_1}}{2} \frac{\partial A_1(0)}{\partial a_2}\right\}, \tag{3.59}$$

$$\frac{\partial N_2}{\partial a_2} = \frac{N_2}{2a_2} + \sqrt{(2a_2)}\left\{\sum_{j=1}^{n_2} (-1)^{j+1} \operatorname{cosec}\left(\frac{2j-1}{4n_2+2}\pi\right) \frac{\partial}{\partial a_2} A_2(s_j) + \frac{(-1)^{n_2}}{2} \frac{\partial A_2(0)}{\partial a_2}\right\}, \tag{3.60}$$

where $(\partial/\partial a_2)A_1(s_i)$ and $(\partial/\partial a_2)A_2(s_j)$ can be determined from the system of simultaneous linear algebraic equations

$$\sum_{i=1}^{n_1} \frac{\partial}{\partial a_2} A_1(s_i) H_1(t_{1i}, y_{1k}; a_1) + \sum_{j=1}^{n_2} \frac{\partial}{\partial a_2} A_2(s_j) H_2(t_{2i}, y_{1k}; a_2)$$

$$= -\sum_{j=1}^{n_2} A_2(s_j) L_2(t_{2j}, y_{1k}), \qquad k = 1, \ldots, n_1, \tag{3.61}$$

$$\sum_{i=1}^{n_1} \frac{\partial}{\partial a_2} A_1(s_i) H_2(t_{1i}, y_{2l}; a_1) + \sum_{j=1}^{n_2} \frac{\partial}{\partial a_2} A_2(s_j) H_1(t_{2j}, y_{2l}; a_2)$$

$$= -\frac{2}{a_2\sqrt{\pi}}\left(\frac{2\sqrt{3}}{\pi\Delta} y_{2l}\right) \exp\left[-\left(\frac{2\sqrt{3}}{\pi\Delta} y_{2l}\right)^2\right] - \frac{a_1}{a_2} \sum_{i=1}^{n_1} A_1(s_i) L_3(t_{1i}, y_{2l})$$

$$- \sum_{j=1}^{n_2} A_2(s_j) L_1(t_{2j}, y_{2l}), \qquad l = 1, \ldots, n_2. \tag{3.62}$$

The values of $\partial A_1(s_i)/\partial a_2$, $\partial A_2(s_j)/\partial a_2$ at $s_i = s_j = 0$ are obtained by interpolation. The functions H_1, H_2, L_1, L_2, L_3 and their arguments in the above equations are given by the relations (3.30), (3.31), (3.34)–(3.36) and (3.49)–(3.54).

4. NUMERICAL RESULTS

In this section we shall illustrate our general results by means of specific numerical examples. Both temperature profiles (2.1) and (2.2) will be used. These will serve to demonstrate two modes of snap-through crack closure phenomena.

Example one

First we shall use temperature profile (2.2) with $n = 0.5$, and set the dimensionless critical stress intensity factor $N_c = 0.15$; this choice is discussed later on in this section.

For a fixed value of $\Delta = \delta/b$, we calculate dimensionless crack lengths, $a_1 = a_2$, such that $N_1 = N_2 = N_c$. Branch ABB' in Fig. 8. is obtained in this manner. This is the fundamental equilibrium path in the Δ, $a_1 = a_2$-space. Not all states on this branch are stable. For states corresponding to the AB portion of this branch, $\partial N_1/\partial a_1 = \partial N_2/\partial a_2 \leq 0$, the equality sign corresponding to the critical state B. Therefore, all states between A and B are stable, and all states between B and B' are unstable, since for these $\partial N_1/\partial a_1 = \partial N_2/\partial a_2 > 0$. Correct to about 0.1%, at the critical state B, We have $\Delta = \Delta_c = 4.586$, and $a_1 = a_2 = a_c = 3.883$.

After point B, crack 1 ceases to grow, while crack 2 continues to extend, as Δ is increased. This leads to the stable branch BB^*, on which $\partial N_2/\partial a_2 < 0$. Along this branch, N_1, as well as $|\partial N_2/\partial a_1|$, continue to decrease monotonically with increasing Δ, as shown in Fig. 9, attaining zero at $\Delta = 5.482$, where $a_2 = 4.900$. At this point, the change in the stress intensity factors is governed by

$$dN_1 = \frac{\partial N_1}{\partial a_1} da_1 + \frac{\partial N_1}{\partial a_2} da_2 + \frac{\partial N_1}{\partial \Delta} d\Delta = 0.103\, da_1 - 0.001\, da_2 - 0.083\, d\Delta,$$

$$dN_2 = \frac{\partial N_2}{\partial a_1} da_1 + \frac{\partial N_2}{\partial a_2} da_2 + \frac{\partial N_2}{\partial \Delta} d\Delta = 0.000\, da_1 - 0.309\, da_2 + 0.266\, d\Delta. \tag{4.1}$$

Now, if we consider an increment $d\Delta > 0$, and choose $da_2 \approx 0.86\, d\Delta$, we will have $dN_2 \approx 0$, so that N_2 remains at the critical value, N_c. On the other hand, for these choices,

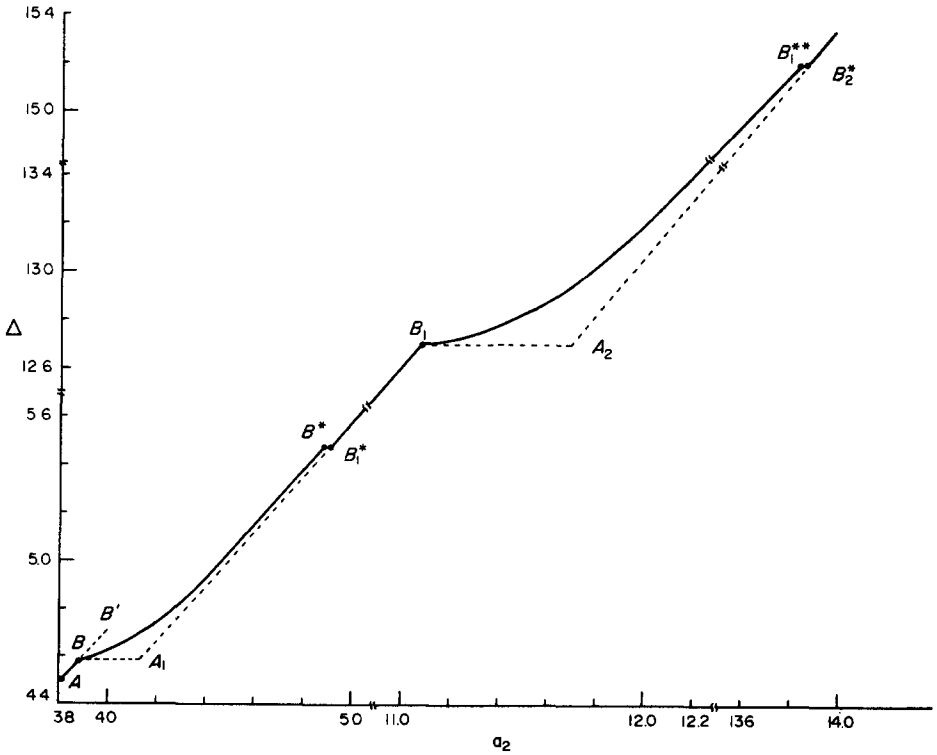

Fig. 8. Variations in crack lengths and crack spacing as functions of the load parameter Δ for temperature profile eqn (2.2) with $n = 0.5$.

and since da_1 cannot be positive (because $N_1 = 0 < N_c$), we observe from (4.1), that $dN_1 < 0$. This means that da_1 must be negative, because N_1 must remain zero, and therefore crack 1 proceeds to close. Further calculations show that this process accelerates spontaneously because, as a_1 decreases, the rate at which N_1 decreases becomes faster. Hence, crack 1 snaps closed as crack 2 extends to a longer length. The crack spacing doubles after this.

Branch A_1B_1 in Fig. 8 corresponds to the state in which every other crack is closed. Hence, the state at point B^* moves horizontally to state B_1^* on branch A_1B_1. This new state is stable. The entire process then continues until point B_1 at which instability initiates again. After this point, every other crack (the cracks are now spaced at distance $2b$) stops growing, and we obtain branch $B_1B_1^{**}$. The state at B_1^{**} is similar to that at B^* discussed before. Hence, after this state the crack spacing changes from $2b$ to $4b$, as every other crack snaps closed. The entire regime continues in such a manner that the crack spacing and the crack depth maintain a somewhat equal order of magnitude.

We note that the stability conditions, $\partial N_1/\partial a_1 < 0$ and $\partial N_2/\partial a_2 < 0$, must not be violated for stable states, as long as the corresponding stress intensity factors are at the critical value, i.e. as long as the corresponding crack is *active*. Therefore, since on branch AB both cracks are active, both of the above inequalities must prevail. On the stable branch BB^*, on the other hand, crack 1 is inactive, $N_1 < N_c$, and therefore $\partial N_1/\partial a_1$ may be positive, while $\partial N_2/\partial a_2$ does and must remain negative. Moreover, the quantity $\partial N_2/\partial a_1$ remains negative as long as N_1 is positive, and it vanishes with vanishing N_1; actually, the curve corresponding to $\partial N_2/\partial a_1$ is tangent to the Δ-axis at the point where N_1 vanishes, see Fig. 9. This occurs at point B^*, and at this point $\partial N_1/\partial a_2$ is unrestricted; see eqn (4.2) below.

Example two

We shall now use the temperature profile given by (2.1), and again set $N_c = 0.15$. The results are shown in Fig. 10. Branches AB and BB^* have similar meanings to the corresponding ones in Fig. 8. However, at point B^* ($\Delta = 3.835$, $a_2 = 1.578$) in Fig. 10 the only stable state which the system can attain is point B_2^* ($\Delta = 3.835$, $a_2 = 2.129$) on branch A_2B_2 which corresponds to the crack spacing of $4b$. This means that if *only* two interacting cracks are considered then, after the state corresponding to B^*, not only those cracks which have stopped growing would snap closed, but also that every other of those cracks that had continued growing would snap closed: the crack spacing quadruples after this state. The entire process then continues.

We should carefully point out that the above result may be due to the fact that we have not considered *three interacting cracks*, as shown in Fig. 11. It may happen that before state B^* in Fig. 10 is reached, crack 3 in Fig. 11 stops growing, after which state every third crack (namely crack 2) would continue to grow. At this stage of the crack development, crack 1 would involve both Modes I and II. We have not analyzed this possibility.† It presents a considerably more difficult problem. However, we expect that eventually both cracks 1 and 3 would snap closed, and that a point on branch B_1A_1 would be attained. However, this is mere (educated) speculation, and only analytical results can establish a reliable conclusion.

On the accuracy of the results. Lacking a rigorous error estimate, we have tried to check the accuracy of our numerical results in three different ways: (1) We have applied the method to problems with known solutions; (2) Since a collocation method is used, we have obtained the same results using several significantly different numbers of collocation points; and (3) We have used the identity

$$N_1 \partial N_1/\partial a_2 = N_2 \partial N_2/\partial a_1. \tag{4.2}$$

The first check is that for the single edge crack solved by Koiter[13], in which the value of stress intensity factor is given exactly as $2N = 1.5861$. Table 1 shows values for stress intensity factors which we have obtained by our analysis for a uniform load and for different numbers of collocation points. The results for forty points appear to differ by about 0.3% from the exact value. Also shown in Table 1 are values for the stress intensity factors using two interpolation

†A complete theory of unstable growth of interacting cracks, involving Modes I, II and III, is given by Nemat-Nasser[12].

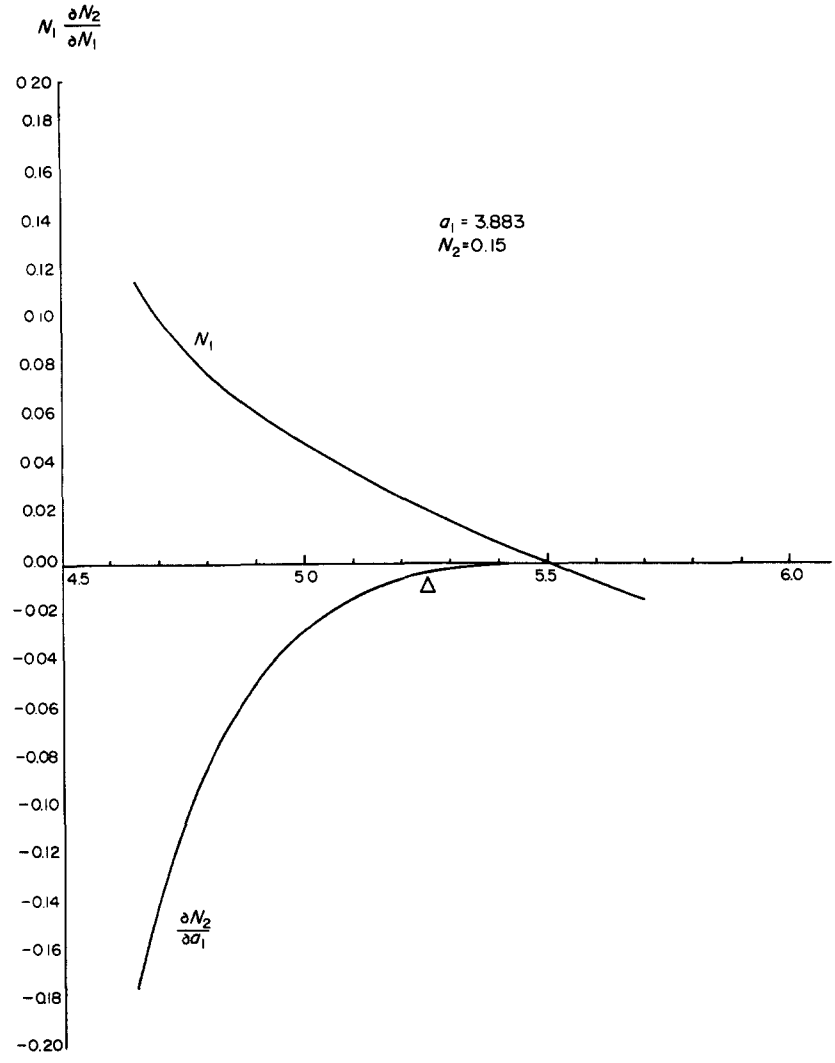

Fig. 9. Variation in dimensionless stress intensity factor N_1 and in $\partial N_2/\partial a_1$ as functions of Δ, on branch BB^* of Fig. 8.

Table 1. Single edge crack

Number of points	2N (Eq. 3.43)	2N (Interpolation)
40	1.5811	1.5818
60	1.5827	1.5832
80	1.5835	1.5839
100	1.5840	1.5844

points. These values were also tested for three and four interpolation points and the results are the same. Thus, if an accurate value for stress intensity factor is desired it is not essential to use eqns (3.43) and (3.44) since interpolation produces adequate results. This is not the case for the derivatives of the stress intensity factors.

Another check was made by specializing the problem to an infinite array of edge cracks of equal lengths. For this case the error function profile was used. The results are given in Table 2 for $\Delta = 1.5$ and $a_1 = a_2 = 1.3229$. It can be seen from this table that while the stress intensity factor is essentially unchanged the derivatives do change significantly with the number of collocation points. One might infer that the error in the derivative is the same for different crack configurations. However, the accuracy of the derivatives will also be seen to depend upon the relative crack length as well as the crack lengths.

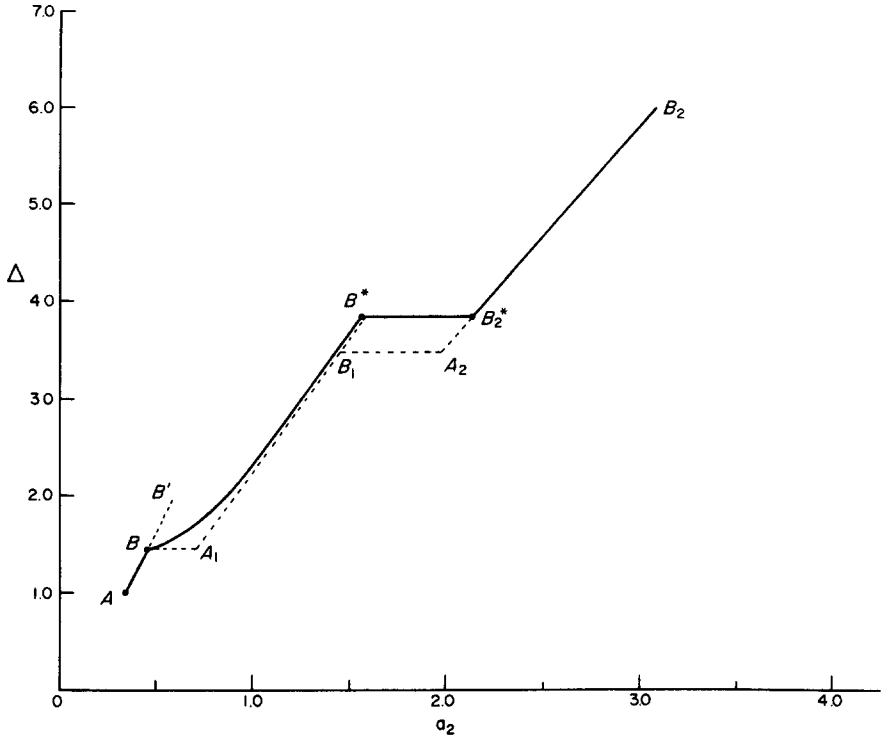

Fig. 10. Variations in crack lengths and crack spacing as functions of the load parameter Δ for temperature profile eqn (2.1).

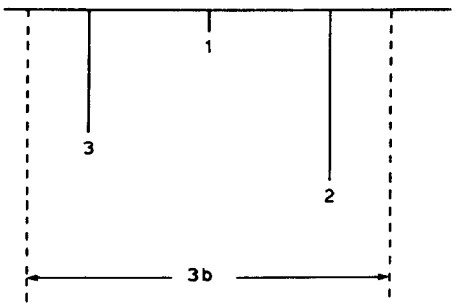

Fig. 11. A unit cell with three unequal cracks: Crack 1 involves both Modes I and II.

Table 2. Infinite array of cracks ($a_1 = a_2 = 1.3229$, $\Delta = 1.5$)

Number of points	$N_1 = N_2$	$\partial N_1/\partial a_2$	$\partial N_2/\partial a_2$
30	0.1501	-0.2966	-0.4380
40	0.1500	-0.2984	-0.4338
50	0.1500	-0.3011	-0.4288
60	0.1500	-0.3016	-0.4299
70	0.1500	-0.3031	-0.4292

For equal cracks, when $a_1 = a_2$ is less than 10, 50 collocation points seem to give better than three significant figure accuracy in the dimensionless stress intensity factors $N_1 = N_2$, and in the crack lengths $a_1 = a_2$. In our calculations the critical points are established using 80 collocation points for each crack. Thus the numerical results are accurate to at least four significant figures for $N_1 = N_2$ and $a_1 = a_2$.

The accuracy in the calculations of the derivatives, $\partial N_i/\partial a_j$, is considerably lower than that for N_i and a_i, and becomes worse as the cracks become more unequal. This feature is seen in

Table 3. Error near critical point ($a_1 = 3.883$, $N_2 = N_c = 0.15$, 40 collocation points)

Δ	a_2	N_1	$\partial N_1/\partial a_1$	$\partial N_1/\partial a_2$	$\partial N_2/\partial a_1$	$\partial N_2/\partial a_2$	Error* ϵ
4.65	4.076946	0.10817	0.08457	-0.24798	-0.17813	-0.17690	0.00010
4.95	4.430745	0.05665	0.12901	-0.10210	-0.03788	-0.30976	0.00010
5.25	4.701950	0.02163	0.12208	-0.02794	-0.00375	-0.31827	0.00004

* $\epsilon = |N_1\ \partial N_1/\partial a_2 - N_2\ \partial N_2/\partial a_1|$.

Table 3, where 40 collocation points were used and where $a_1 = 3.883$, $N_2 = N_c = 0.15$. Equation (4.2) provides an excellent check for the consistency of the results when the cracks are unequal, as long as N_1 is positive. The error $\epsilon = |N_1\,\partial N_1/\partial a_2 - N_2\,\partial N_2/\partial a_1|$ is given in Table 3 for three cases and it appears to be consistent in magnitude.

It should be pointed out that the stability calculations require quantities that are not usually calculated in fracture analysis, namely the derivatives of the stress intensity factors with respect to crack lengths. Consequently, there is a requirement for higher accuracy than is usually obtained by numerical techniques. The authors doubt that recent finite element work, even that using special elements, will prove adequate for such analyses. In fact, considerable effort is required to develop analytical tools to obtain these quantities with reasonable accuracy.

Minimum crack spacing. To estimate the initial crack spacing, we observe that before cracking, the total strain energy per unit thickness, in a strip of length b, is given by (for temperature profile eqn 2.1)

$$W = \frac{1}{2}\hat{\alpha}^2 T_0^2 b \frac{E}{1-2\nu}\int_0^\infty \left[1 - \operatorname{erf}\left(\frac{y\sqrt{3}}{\delta}\right)\right]^2 \mathrm{d}y. \tag{4.3}$$

To simplify the calculation, we approximate the temperature profile $\hat{T} = T - T_0$ by a parabolic curve $\hat{T} = T_0(1 - y/\delta)^2$ which satisfies the boundary condition at $y = 0$, and together with its gradient vanishes at $y = \delta$. Equation (4.3) then becomes

$$W \simeq \frac{1}{2}\hat{\alpha}^2 T_0^2 b \frac{E}{1-2\nu}\int_0^\delta (1 - y/\delta)^4\,\mathrm{d}y = \frac{1}{10}\alpha^2 T_0^2 b\delta \frac{E}{1-2\nu}. \tag{4.4}$$

Let θ be the fraction of this strain energy which is used to generate new surfaces as the thernal cracks initially form. If h is the crack length, we must have

$$\frac{\theta}{10}\hat{\alpha}^2 T_0^2 b\delta \frac{E}{1-2\nu} = 2h\gamma. \tag{4.5}$$

From this equation, we obtain

$$b = \frac{20(1-2\nu)h\gamma}{\theta\hat{\alpha}^2 T_0^2 \delta E}. \tag{4.6}$$

We now substitute from (4.6) into (3.32), note that $k_c = K_c/\sqrt{(2\pi)} = [\gamma E/\pi(1-\nu^2)]^{1/2}$ and $\hat{\beta} = \hat{\alpha}E/(1-2\nu)$, and arrive at

$$N_c \simeq \left[\frac{\theta\delta(1-2\nu)}{20\,h\pi(1-\nu^2)}\right]^{1/2}. \tag{4.7}$$

It is interesting to note that this *estimate* does not depend on the temperature change T_0 and on the elastic modulus E. Note, however, that it is the constant value K_c, and not N_c, which the stress intensity factor must attain at the crack tip as the crack grows. N_c, therefore, will change as the crack spacing changes, while K_c remains constant (for the ideal brittle material considered here).

For a numerical value, set $\delta \approx h$ and, with $\theta = (1/3)$, obtain $N_c = 0.05$. On the other hand, if $\delta \approx 3h$, and $\theta = 1$, we obtain $N_c = 0.15$.

It should be pointed out that there is an upper value that N_c cannot exceed for a given temperature profile. From the definition of N_c, namely $N_c = K_c/[\sqrt{(2\pi)}\hat{\beta}T_0 b^{1/2}]$, for a given T_0, this places another restriction on the minimum value that crack spacing b can attain. This restriction corresponds to the question of stability. For example for the temperature profile (2.1), and for $\Delta = 1$, the maximum value for N_c that can be attained with $\partial N_1/\partial a_1 = \partial N_2/\partial a_2 \leq 0$, is $N_c \approx 0.19$. If we require that N_c be larger than this number, we cannot have a stable regime. Hence, for a given temperature profile and with Δ fixed, there is an absolute upper value that N_c can possibly attain. However, this upper value is much larger than the upper value corresponding to the stability requirement. For example, for temperature profile (2.1) and with $\Delta = 1$ and $a_1 = a_2 = 0.15$, we will have $N_1 = N_2 = 0.21$, for which $\partial N_1/\partial a_1 = \partial N_2/\partial a_2 = +0.3$, which is unstable; if such a statement can be achieved by imposing certain constraints, then when the constraints are removed, some of the crack would snap closed, which means that the dimensionless stress intensity factor would be reduced.

Acknowledgements—This work was supported in part by the U.S. National Science Foundation under Grant AER 75-00187. The authors are very grateful to Mr. A. Oranratnachai who performed all numerical calculations given herein; the basic theory was originally given in Ref. [14] and also in Section 5 of Ref. [15].

REFERENCES

1. M. C. Smith, R. Potter, D. Brown and R. L. Aamodt, Induction growth of fractures in hot rock. In *Geothermal Energy* (Edited by P. Kruger and C. Otto), p. 251. Stanford University Press (1973).
2. C. E. Pearson, General theory of elastic stability. *Q. Appl. Math.* **14**, 133 (1956).
3. R. Hill, On uniqueness and stability in finite elastic strain. *J. Mech. Phys. Solids* **5**, 229 (1957).
4. S. Nemat-Nasser, On thermomechanics of elastic stability. *Z. Angew. Math. Phys.* **21**, 538 (1970).
5. J. M. T. Thompson and G. W. Hunt, *A General Theory of Elastic Stability*. Wiley, New York (1973).
6. J. Roorda, Concepts in elastic structural stability. In *Mechanics Today* (Edited by S. Nemat-Nasser Vol. 1, p. 322. Pergamon Press, Oxford (1974).
7. J. F. Knott, *Fundamentals of Fracture Mechanics*. Butterworth, London (1973).
8. L. M. Keer and K. Chantaramungkorn, An elastic half plane weakened by a rectangular trench. *J. Appl. Mech.* **42**, 683 (1975).
9. I. S. Gradshteyn and I. M. Rhyzhik, *Tables of Integrals Series and Products*. Academic Press, New York (1965).
10. F. Erdogan, G. D. Gupta and T. S. Cook, Numerical solution of singular integral equations. In *Methods of Analysis and Solutions of Crack Problems* (Edited by G. C. Sih), p. 368. Noordhoff, Holland (1972).
11. S. Krenk, On the use of the interpolation polynomial for solutions of singular integral equations. *Q. Appl. Math.* **32**, 479 (1975).
12. S. Nemat-Nasser, Stability of a system of interacting cracks in combined modes. June 1977, to appear in *Int. J. Engng Sci., Letters in Appl. Engng Sci.* preprint: Earthquake Research and Engineering Lab., Dept. of Civil Engineering, Northwestern University (July 1977).
13. W. T. Koiter, Rectangular tensile sheet with symmetric edge cracks. *J. Appl. Mech.* **32**, 237 (1965).
14. L. M. Keer, S. Nemat-Nasser and K. S. Parihar, Growth and stability of thermally induced cracks in brittle solids. Northwestern University Geothermal Energy Research Project (Sept. 1976).
15. S. Nemat-Nasser, Overview of the basic progress in ductile fracture. In *Trans. 4th Int. Conf. Struct. Mech. in Reactor Tech.*, Vol. L, paper L2/1 (Aug. 1977).